Cellular Physiology and Biochemistry

Cell Physiol Biochem 2018;46:1112-1121
DOI: 10.1159/000488840
Published online: April 18, 2018
Accepted: February 27, 2018

Original Paper

Characterization of the σ-Pore in Mutant *h*K_v1.3 Potassium Channels

Pavel Tyutyaev Stephan Grissmer

Institute of Applied Physiology, Ulm University, Ulm, Germany

Key Words
Potassium channel • K_v1.3 channel • σ-pore • Electrophysiology • Patch-clamp

Abstract
Background/Aims: The replacement of the amino acid valine at position 388 (*Shaker* position 438) in *h*K_v1.3 channels or at the homologue position 370 in *h*K_v1.2 channels resulted in a channel with two different ion conducting pathways: One pathway was the central, potassium-selective α-pore, that was sensitive to block by peptide toxins (CTX or KTX in the *h*K_v1.3_V388C channel and CTX or MTX in the *h*K_v1.2_V370C channel). The other pathway (σ-pore) was behind the central α-pore creating an inward current at potentials more negative than -100 mV, a potential range where the central α-pore was closed. In addition, current through the σ-pore could not be reduced by CTX, KTX or MTX in the *h*K_v1.3_V388C or the *h*K_v1.2_V370C channel, respectively. ***Methods:*** For a more detailed characterization of the σ-pore, we created a trimer consisting of three *h*K_v1.3_V388C α-subunits linked together and characterized current through this trimeric *h*K_v1.3_V388C channel. Additionally, we determined which amino acids line the σ-pore in the tetrameric *h*K_v1.3_V388C channel by replacing single amino acids in the tetrameric *h*K_v1.3_V388C mutant channel that could be involved in σ-pore formation. ***Results:*** Overexpression of the trimeric *h*K_v1.3_V388C channel in COS-7 cells yielded typical σ-pore currents at potentials more negative than -100 mV similar to what was observed for the tetrameric *h*K_v1.3_V388C channel. Electrophysiological properties of the trimeric and tetrameric channel were similar: currents could be observed at potentials more negative than -100 mV, were not carried by protons or chloride ions, and could not be reduced by peptide toxins (CTX, MTX) or TEA. The σ-pore was mostly permeable to Na^+ and Li^+. In addition, in our site-directed mutagenesis experiments, we created a number of new double mutant channels in the tetrameric *h*K_v1.3_V388C background channel. Two of these tetrameric double mutant channels (*h*K_v1.3_V388C_T392Y and *h*K_v1.3_V388C_Y395W) did not show currents through the σ-pore. ***Conclusions:*** From our experiments with the trimeric *h*K_v1.3_V388C channel we conclude that the σ-pore exists in *h*K_v1.3_V388C channels independently of the α-pore. From our site-directed mutagenesis experiments in the tetrameric *h*K_v1.3_V388C channel we conclude that amino acid position 392 and 395 (*Shaker* position 442 and 445) line the σ-pore.

Stephan Grisssmer
Ulm University, Institute of Applied Physiology
Albert-Einstein-Allee 11, Ulm, Germany
Tel. +49 731 500 23253, Fax +49 731 500 36202, E-Mail stephan.grissmer@uni-ulm.de

Introduction

K_v1.2 and K_v1.3 channels belong to the family of the voltage-gated potassium channels which comprises a big number of ion channels with diverse functions. The functional channel is formed by the assembly of four subunits. The single subunit contains six transmembrane domains (S1-S6), with a conserved P region. The residues connecting segments S5 and S6 of each subunit form the central, ion-selective pore of the channel. The segments S1-S4 form the voltage-sensing domain (VSD) controlling the gates [1, 2]. The N- and C-terminals of the channel protein are located on the intracellular side [3].

Mutations in the VSD of the voltage-gated Na_v1.2 channel or in the voltage-gated *Shaker* potassium channel resulted in the formation of another ion permeation pathway through the channel molecule [2, 4-7], termed ω-pore. Currents through the ω-pore were selective for monovalent cations and could be measured at potentials at which the α-pore was closed [2]. Many studies showed that substituting residues in the VSD influenced the selectivity of the ω-pore in potassium channels and that the ω-current could either be carried by protons or cations [8]. All of these mutations were located in the transmembrane S4 segments and neutralized positive charges important for voltage sensitivity [9].

A different ion conducting pathway, the σ-pore, was described in mutant voltage-gated potassium channels in which a valine was replaced by a cysteine at position 388 in *h*K_v1.3 channels (*Shaker* position 438) or at the homologue position 370 in *h*K_v1.2 channels [10, 11]. This mutation showed, in addition to the current through the central, potassium-selective α-pore, an additional inward current at membrane potentials more negative than -100 mV, i.e. at potentials where the α-pore is normally closed. The inward current of the mutant channel was similar but not identical to the ω-current in the VSD-mutant channels, for example, Na^+ and Li^+ could carry large inward σ-current whereas ions like K^+ and Rb^+ only generated small inward σ-currents [10, 11]. In addition, current through the σ-pore was blocked by verapamil and not influenced by CTX, KTX or MTX [10, 11]. According to the model of the mutant *h*Kv1.3_V388C channel [10], the σ-pore was located behind the central α-pore at the back of the selectivity filter and proceeded in parallel to the central α-pore. The entry of the σ-pore from the extracellular side was assumed to be located at the backside of Y395 (*Shaker* position 445) of the GYG-motif and F384 (*Shaker* position 434) of the pore helix. It seemed that a single σ-pore forms between two neighboring S6 subunits and it runs parallel to the central α-pore.

The goal of this study was to confirm the existence of the σ-pore in trimeric *h*Kv1.3_V388C mutant channels and to identify amino acids in the tetrameric channels that form the σ-pore.

Materials and Methods

Molecular cloning and site directed mutagenesis

The *h*Kv1.3_wt construct (a generous gift from Prof. Dr. O. Pongs, Institute for Neural Signal Processing, Center for Molecular Neurobiology, Hamburg Germany) was cloned in the pRc/CMV vector (Invitrogen, San Diego, USA). The following strategy was selected for creating the *h*K_v1.3_V388C_trimeric channel: we linked three *h*K_v1.3_V388C mutant subunits, each linker consisted of three alanines. This newly created *h*K_v1.3_V388C_trimer was cloned into the pcDNA3 vector with EGFP at the C-terminus.

To test which amino acids in the tetrameric *h*K_v1.3_V388C channel line the σ-pore pathway, we introduced additional mutations in the *h*K_v1.3_V388C mutant channel thus creating double mutant channels. The rational for this approach was to replace the side chains of those amino acids that might be involved in the formation of the σ-pore with larger side chains. If these amino acids were part of the σ-pore, these modifications might stop the flow of current through the σ-pore. As a control,

Table 1. List of mutations to test the σ-pore

Background channel	Substitution
hK_v1.3_V388C	M390F
	A413F
	Y395W
	W384F
	T392Y
	V393L

the same sites were mutated in the *h*Kv1.3_wt channel (see Tab. 1). The new mutant *h*K_v1.3 channels used in this study were created by site-directed mutagenesis (Eurofins Genomics GmbH, Ebersberg, Germany), confirmed by sequencing (Eurofins Genomics GmbH, Ebersberg, Germany) and amplified in *E*. coli.

Cell culture

The cell line COS-7 (DSMZ no. ACC 60, Braunschweig, Germany) was grown in DMEM (Gibco, Paisley, UK), supplemented with 10 % fetal bovine serum (Sigma, Mannheim, Germany). Cells were kept in a humidified atmosphere at 37°C and 5 % CO_2. Cells were transfected using the FuGENE 6® transfection reagent (Roche Molecular Biochemicals, Mannheim, Germany) with 1 µg of pEGFP-C3 (Clontech, Mountain View, USA) DNA and 5 µg of mutant potassium channel DNA. COS-7 cells were used as our expression system because they express low levels of endogenous ion channels. Cells were viewed with an inverted fluorescence microscope (Zeiss, Oberkochen, Germany). The transfected cells were plated the day after transfection on poly-L-lysine-coated coverslips, and EGFP-positive cells were patch clamped 36-48 h after transfection, as described below.

Electrophysiological recordings

The measurements were performed on a vibration-isolation table (Newport Corporation, Irvine, USA) equipped with an inverted microscope Axiovert 25 (Carl Zeiss AG, Jena, Germany) with xenon lamp and fluorescence detection unit. A Dell computer running Patchmaster 2.0 data acquisition software was connected to the EPC-9 amplifier (HEKA Elektronik GmbH, Lambrecht, Germany). All experiments were performed using the whole-cell recording mode of the patch-clamp technique at room temperature 19-22°C [12, 13]. Currents were filtered through a 2.9 kHz Bessel Filter and capacitative and leakage currents were not subtracted. All voltage ramp protocols were preceded by a 100-ms prepulse to the starting potential to avoid complications associated with the slow „activation" of the σ-current. The analysis of the data was performed with the programs Fitmaster v2.15 (HEKA Elektronik GmbH) and Igor Pro 3.1.2 v. 7.01 (Wave Metrics Inc., Lake Oswego, Oregon). Patch electrodes were pulled from thin-walled, single-filament borosilicate glass (1.5 mm outer diameter; Science products GmbH, Hofheim, Germany) using a microelectrode puller (DMZ universal puller, Martinsried, Germany). Pipette tip resistances ranged from 1 to 3 MΩ and seal resistances were >1 GΩ.

Solution and Chemicals

The external bathing solution for current measurements consisted for $[4.5\ K^+]_o$ (in mM): 160 NaCl, 4.5 KCl, 2 $CaCl_2$, 1 $MgCl_2$, 5 HEPES with the pH adjusted to 7.4 with NaOH; $[X^+]_o$ (in mM): 164.5 XCl, 2 $CaCl_2$, 1 $MgCl_2$, 5 HEPES adjusted to pH 7.4 with XOH, X stands for K^+, Rb^+, Cs^+, Li^+ and NH_4^+. The osmolarity of the bathing solutions was 300-310 mOsm. The internal pipette solution consisted of (in mM) 145 KF, 2 $MgCl_2$, 10 HEPES, 10 EGTA adjusted to pH 7.2 with KOH and the osmolarity was 310 mOsm. Charybdotoxin, CTX (Bachem, Bubendorf, Switzerland) was dissolved in a bathing solution containing 0.1 % bovine serum albumin, BSA (Sigma, St. Louis, USA). All other reagents were obtained from Sigma (Mannheim, Germany).

Modeling

Through homology modeling we created a 3-D model of the *h*K_v1.3_wt using the *h*K_v1.2_wt (2A79) template in combination with the Yasara program (www.yasara.org). We changed the valine at position 388 in the *h*K_v1.3_wt monomer into a cysteine with the help of the Deep Viewer software (Swiss PDB viewer, Expasy Server) followed by the creation of the *h*K_v1.3_V388C homotetramer. The σ-pore was simulated using the CAVER software (Loschmidt Laboratories, http://www.caver.cz) and visualized with the PyMOL viewer (DeLano Scientific LLC, Schrödinger).

Results

To test the σ-current pathway, we used two different approaches: First, we created a trimeric *h*K_v1.3_V388C channel that might structurally be able to provide a functional σ-pore and might not be sufficient to form a central α-pore. Second, we created a variety of double mutants of the tetrameric *h*K_v1.3_V388C mutant channel to analyze which amino acid position - that might be involved in the formation of the σ-pore - might hinder current flow through the σ-pore. The results of these two approaches are presented below.

Current through the σ-pore in $hK_v1.3$_V388C mutant tetrameric channels

Fig. 1 shows typical ramp currents of a cell transfected only with EGFP (Fig. 1*A*) in bathing solutions containing either 4.5 (black trace) or 164.5 mM $[K^+]_o$ (red trace). No significant difference between the ramp currents in the different solutions can be observed. The EGFP-transfected COS-7 cell had very small endogenous currents at potentials more negative than -10 mV with little outward current at potentials more positive than +10 mV. In comparison to the current through only EGFP-transfected cells, the currents through cells transfected with $hK_v1.3$_wt channels showed the expected behavior as described earlier [10] and demonstrated here in Fig. 1*B* in 4.5 and 164.5 mM $[K^+]_o$ bathing solutions. Only tiny currents, presumably reflecting leak current, were observed at potentials more negative than -60 mV because the $hK_v1.3$_wt channels were closed. As soon as $hK_v1.3$_wt channels open at potentials more positive than -40 mV a large outward current could be observed in $[4.5\ K^+]_o$ and an inward current in $[164.5\ K^+]_o$ that reversed direction and turned into an outward current around 0 mV.

Experiments with the mutant $hK_v1.3$_V388C tetrameric channel (Fig. 1*C*) showed large inward currents at potentials ranging from -200 to -60 mV in $[4.5\ K^+]_o$ bathing solution. This inward current (Fig. 1*C*, black trace) was expected from earlier experiments using this channel mutant [10] and was due to current flowing through the σ-pore. Since current flow through the σ-pore was reported to be prevented in solutions containing high external K^+ [10], it was no surprise that in 164.5 mM $[K^+]_o$ at the same potential range, the inward current decreased (Fig. 1*C*, red trace) and the ramp current looked similar to the ramp current in the $hK_v1.3$_wt (compare Fig. 1*B*) with an inward current dip at ~ -40 mV indicating current flow through the central potassium-selective α-pore. To measure more precisely the kinetic behavior of the current through the α- and σ-pore simultaneously we performed measurements using voltage steps similar to those described before [10, 11] and shown in Fig. 1*D-F*.

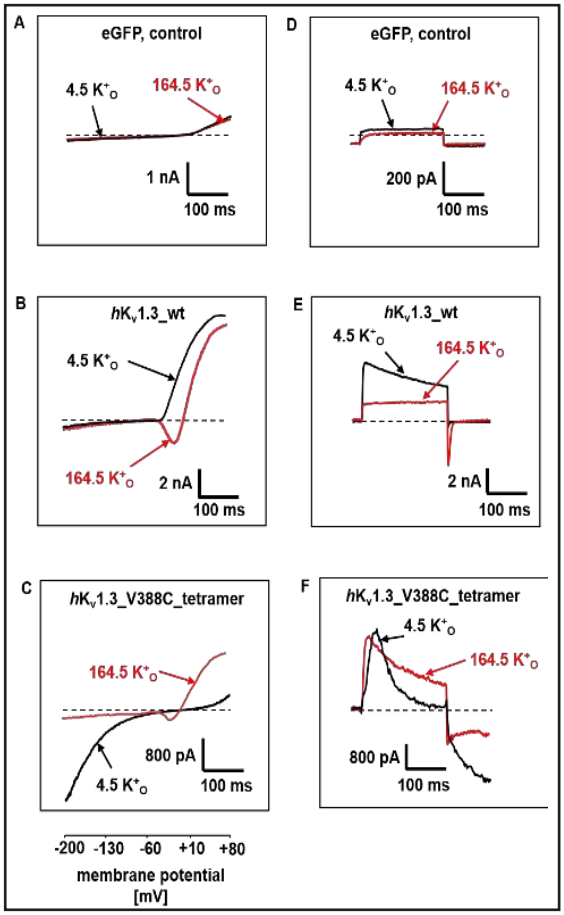

Fig. 1. Tetrameric $hK_v1.3$_V388C mutant channels promote an inward current at potentials more negative than -100 mV. A-C, Ramp currents through control-transfected (eGFP) COS-7 cells (A), $hK_v1.3$_wt (B), and $hK_v1.3$_V388C (C) tetrameric channels in $[4.5\ K^+]$ (black traces) and $[164.5\ K^+]_o$ (red traces) external bathing solution. The currents were elicited with 400-ms voltage ramps from -200 to +80 mV every 30 s from a holding potential of -100 mV. D-F, Currents through control-transfected (eGFP) COS-7 cells (D), $hK_v1.3$_wt (E), and $hK_v1.3$_V388C (F) tetrameric channels were elicited with 100-ms depolarizing pulses from the holding potential of –120 to +40 mV followed by 100 ms hyperpolarizing pulses to –180 mV in $[4.5\ K^+]$ (black traces) and in $[164.5\ K^+]$ (red traces) external bathing solution.

As expected we observed in the *h*Kv1.3_V388C mutant channel in $[4.5\ K^+]_o$ (Fig. 1*F*, black trace) an outward current at +40 mV through the α-pore that inactivated ~10-fold faster than in wild-type as shown in Fig. 1*E* (black trace) and an inward current at -180 mV. In comparison, current through the *h*Kv1.3_V388C mutant channels in $[164.5\ K^+]_o$ (Fig. 1*F*, red trace) showed slower inactivation at +40 mV compared with that in $[4.5\ K^+]_o$ (Fig. 1*F*, black trace). The records shown in Fig. 1 confirm the experiments presented earlier [10] indicating that the V388C mutation in *h*Kv1.3 generated a tetrameric channel with two ion-conducting pathways. One, the central α-pore allowing the flux of K^+ in the presence of K^+, and a second pathway, the σ-pore that runs behind the selectivity filter between two neighboring S6-segments.

σ-pore-like currents can be observed in the trimeric $hK_v1.3$_V388C channel

In order to further confirm the existence of the σ-pore, a trimeric $hK_v1.3$_V388C channel was generated to see if σ-like currents could be observed since in a trimeric $hK_v1.3$_V388C channel, S6-segments might still be able to interact with each other, however, a central α-pore should not exist. The experiments using these trimeric $hK_v1.3$_V388C mutant channels are shown in Fig. 2 demonstrating ramp currents (Fig. 2*A*) and currents elicited with voltage steps (Fig. 2*B*) through $hK_v1.3$_V388C_trimeric mutant channels in bathing solutions containing either 4.5 (black traces) or 164.5 mM $[K^+]_o$ (red traces). Inward currents through $hK_v1.3$_V388C trimeric channels at potentials more negative than -60 mV in a bathing solution containing 4.5 mM $[K^+]$ (Fig. 2*A*, black trace) were large and similar to currents through tetrameric $hK_v1.3$_V388C channels (compare Fig. 1*C*, black trace) indicating that σ-like currents can be observed in trimeric $hK_v1.3$_V388C channels.

That this inward current through trimeric $hK_v1.3$_V388C channels was due to current flowing through the σ-pore was further confirmed by the reduction of the inward current in a solution with 164.5 $[K^+]_o$ (Fig. 2*A*, red trace), a known property of current through the σ-pore. In addition and as expected, the ramp current in 164.5 $[K^+]_o$ (Fig. 2*A*, red trace) did not show an inward current dip at ~-40 mV indicating the lack of a functional voltage-dependent potassium-selective α-pore in cells transfected with the trimeric $hK_v1.3$_V388C channels. This assumption was confirmed by measurements using voltage steps (Fig. 2*B*), where little outward current could be observed at +40 mV in either $[4.5\ K^+]_o$ (black trace) or $[164.5\ K^+]_o$ (red trace) with an inward current at -180 mV that was larger in $[4.5\ K^+]_o$ compared to $[164.5\ K^+]_o$ as expected for current through the σ-pore. In further experiments we characterized this current through the trimeric $hK_v1.3$_V388C channels in more detail as shown below.

σ-currents through trimeric $hK_v1.3$_V388C channels were not inhibited by CTX

Application of 700 nM CTX in a bathing solution containing $[4.5\ K^+]_o$ had no effect on ramp currents through trimeric $hK_v1.3$_V388C channels elicited with 400-ms voltage ramps

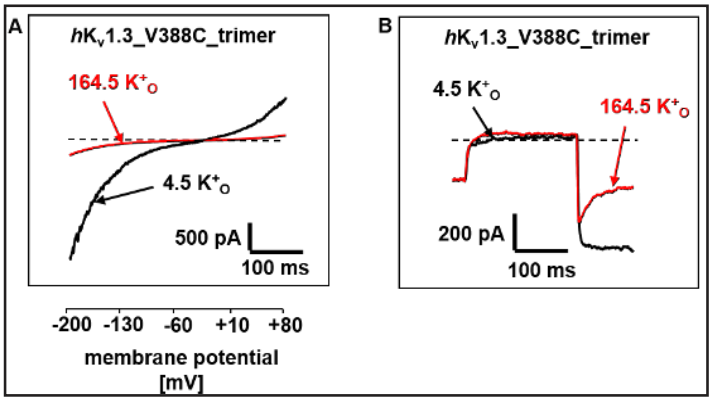

Fig. 2. Characteristic of inward currents in the trimeric $hK_v1.3$_V388C channel. A, ramp currents through trimeric $hK_v1.3$_V388C channels were elicited with 400-ms voltage ramps from -200 to +80 mV from the holding potential of –100 mV in $[4.5\ K^+]_o$ (black traces) and in $[164.5\ K^+]_o$ (red traces) external bathing solution. B, currents through trimeric $hK_v1.3$_V388C channels were elicited with 100-ms depolarizing pulses from the holding potential of –120 to +40 mV followed by 100 ms hyperpolarizing pulses to –180 mV in $[4.5\ K^+]_o$ (black traces) and in $[164.5\ K^+]_o$ (red traces) external bath solution.

from -200 to +80 mV as shown in Fig. 3*A*. It is obvious that the current traces in the absence (black trace) and presence (red trace) of 700 nM CTX are almost identical indicating that CTX cannot block current through the σ-pore of the trimeric $hK_v1.3$_V388C mutant channel similar to the lack of CTX to block current through the σ-pore of the tetrameric $hK_v1.3$_V388C mutant channels [10]. In further experiments we compared the ion selectivity of the σ-current in the trimeric and tetrameric $hK_v1.3$_V388C channels.

Ion selectivity of the σ-current in the trimeric and tetrameric $hK_v1.3$_V388C channels

To find out which ions could permeate through the σ-pore of the tetrameric (Fig. 3*B*) and trimeric $hK_v1.3$_V388C (Fig. 3*C*) mutant channels we replaced the major cation Na^+ in the external bathing solution with Rb^+, K^+, Cs^+, NH_4^+ or Li^+. As described earlier [10] and shown here in Fig. 3*B* the replacement of Na^+ with Li^+ slightly increased the inward current amplitude through the $hK_v1.3$_V388C mutant tetrameric channel whereas the replacement of Na^+ with NH_4^+ or Cs^+ reduced the amplitude of the σ-current and K^+ and Rb^+ generated the smallest σ-currents. Using the amplitudes (I_X^+) of the ramp currents at –180 mV we calculated the ratios (I_X^+/I_{Na}^+) as a measure of ion conductance yielding ion permeation efficiencies similar to those measured earlier [10] for current through the tetrameric $hK_v1.3$_V388C mutant channels relative to Na^+ to be in the following order: Li^+ (1.1) > Na^+ (1) > NH_4^+ (0.8) > Cs^+ (0.69) > K^+ (0.14) > Rb^+ (0.11).

Replacing the major cation in the bathing solution using the trimeric $hK_v1.3$_V388C mutant channels showed similar results as described for current through the σ-pore of the tetrameric $hK_v1.3$_V388C mutant channels (compare Fig. 3*B* and 3*C*). The measurements resulted in an ion permeation efficiency for current through the trimeric $hK_v1.3$_V388C mutant channels in the following order: Li^+(1.2)>Na^+(1)>NH_4^+(0.75)>Cs^+(0.73)>K^+(0.32)> Rb^+(0.12).

Effects of mutations in the presumed σ-pore pathway

To test the σ-pore pathway we introduced additional mutations into the tetrameric $hK_v1.3$_V388C mutant channel in order to see if the second mutation could prevent current flow through the σ-pore. Currents through two of these double mutant channels are shown in Fig. 4*A* and 4*C* for the $hK_v1.3$_V388C/M390F mutant channel and in Fig. 4*B* and 4*D* for the $hK_v1.3$_V388C/Y395W mutant channel. Currents through the double mutant $hK_v1.3$_V388C/M390F channels (Fig. 4*A* and 4*C*) were similar to currents through the single mutant $hK_v1.3$_V388C channels shown in Fig. 1*C* and 1*F* indicating that the σ-pore in this double mutant channel was not blocked although the methionine at position 390 was replaced by the bulky amino acid phenylalanine. In contrast, the currents through the double mutant $hK_v1.3$_V388C/Y395W channels (Fig. 4*B* and 4*D*) were similar to currents through the wild type $hK_v1.3$ channels shown in Fig. 1*B* and 1*E* indicating that the σ-pore in this

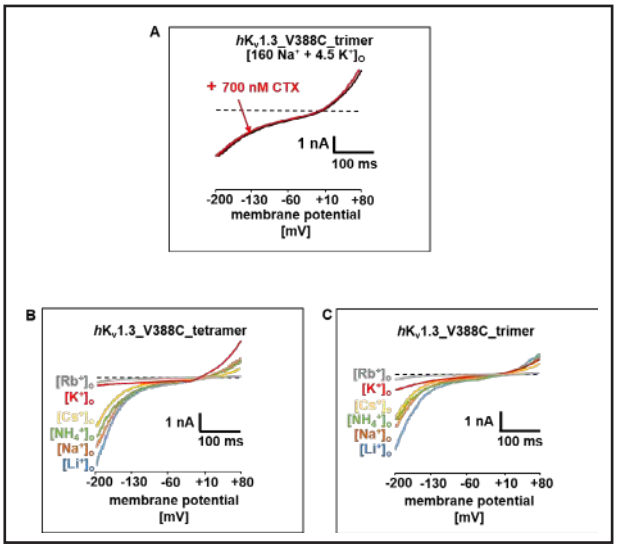

Fig. 3. Properties of current through trimeric and tetrameric $hK_v1.3$_V388C channels. A, currents were elicited with 400-ms voltage ramps from -200 to +80 mV every 30 s from a holding potential of -100 mV under control condition (black trace) and in the presence of 700 nM CTX (red trace). B-C, ion conduction in the tetrameric (B) and the trimeric (C) *h*Kv1.3_V388C channel. The main cations in the external bathing solution are shown at each current trace.

double mutant channel was prevented. This suggested to us that position 395 is directly lining the σ-pore since the replacement of the tyrosine with the very bulky tryptophan prevented current flow through the σ-pore.

Table 2 summarizes the results of these and similar experiments with all double mutants investigated. All the double mutants with the exception of the *h*K$_v$1.3_V388C/W384F channel showed currents through the α-pore and two of the double mutants did not show currents through the σ-pore indicating that these two positions (392 and 395) directly line the σ-pore.

Model of the σ-pore

We modelled the σ-pore of the *h*K$_v$1.3_V388C mutant channel similar to what was described in [10] and according to their model postulate that the entrance of the σ-pore from the outside should be located between Y395 (*Shaker* position 445) on the backside of the central α-pore and W384 (*Shaker* position 434) of the channel as shown in Fig. 5. The model postulates that the σ-pore was opened through the replacement of the valine at position 388 by the smaller amino acid cysteine. This replacement created a larger space between Y395 and W384, which now allows the passage of ions.

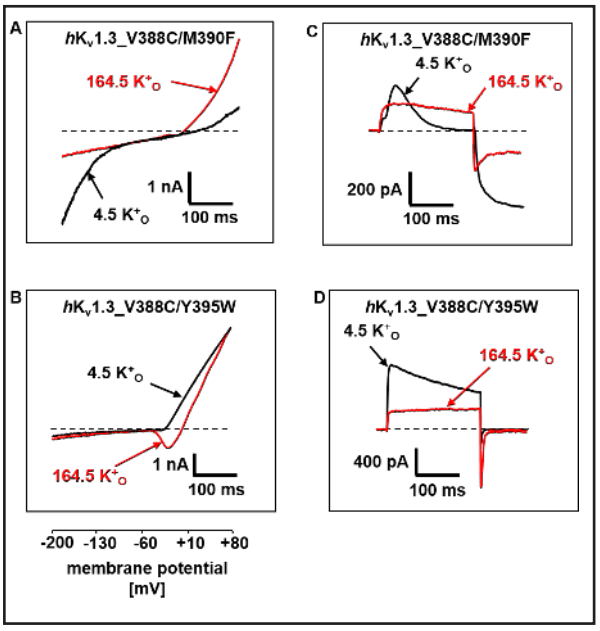

Fig. 4. Double mutant channels that can (*h*K$_v$1.3_V388C_M390F) or cannot (*h*K$_v$1.3_V388C_Y395W) promote a σ-current. A-B, ramp current through the two double mutant tetrameric channels in [4.5 K$^+$]$_o$ (black trace) and [164.5 K$^+$]$_o$ (red trace) external bath solution. The currents were elicited with 400-ms voltage ramps from -200 to +80 mV every 30 s from a holding potential of -100 mV. C-D, currents through *h*K$_v$1.3_V388C_M390F (C) and *h*K$_v$1.3_V388C_Y395W (D) tetrameric channels were elicited with 100-ms depolarizing pulses from the holding potential of –120 to +40 mV followed by 100 ms hyperpolarizing pulses to -180 mV in [4.5 K$^+$]$_o$ (black traces) and in [164.5 K$^+$]$_o$ (red traces) external bathing solution.

Table 2. The tetrameric double mutant channels with and without σ- and α-pores

Channel	Substitution	α-pore	σ-pore
	M390F	+	+
	A413F	+	+
	Y395W	+	-
	T392Y	+	-
*h*Kv1.3_V388C	W384F	-	+
	V393L	+	+

Discussion

The creation of a trimeric *h*K$_v$1.3_V388C mutant channel resulted in typical σ-pore currents at potentials more negative than -100 mV similar to currents observed in the tetrameric *h*K$_v$1.3_V388C mutant channel indicating that the σ-pore was functional in the trimeric mutant channel. In addition, site-directed mutagenesis of amino acids in the tetrameric *h*K$_v$1.3_V388C mutant channel identified two mutant channels (*h*K$_v$1.3_V388C_T392Y and *h*K$_v$1.3_V388C_Y395W) that showed no current through the σ-pore implying that these positions are lining the σ-pore.

Position 390 and 413 in the tetrameric hK$_v$1.3_V388C mutant channel do not interfere with the σ-pore

According to the model shown in Fig. 6*A*, position 390 cannot influence the σ-pore. Both residues, methionine or phenylalanine (M390F), run parallel to the σ-pore and do

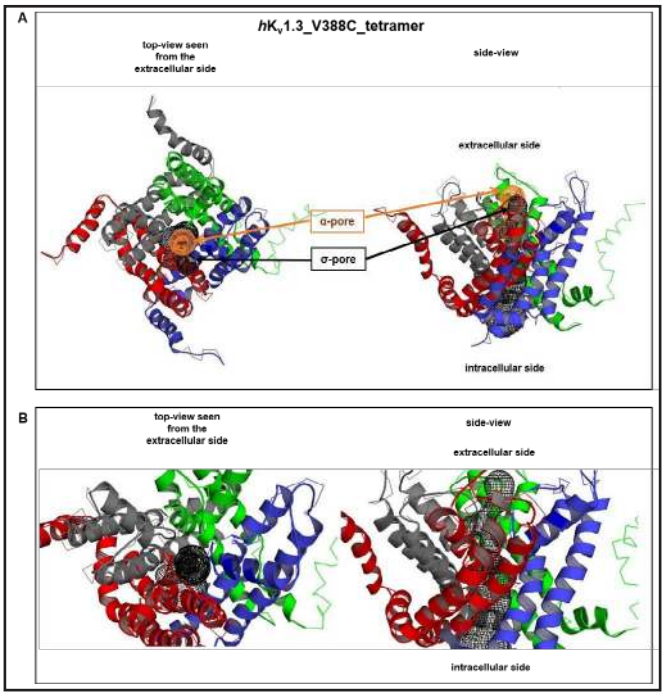

Fig. 5. Proposed σ-pore pathway through the tetrameric *h*K$_v$1.3_V388C mutant channel. The σ-pore is shown in black, the α-pore is shown in orange. (A), overview of the σ- and α-pore in the *h*K$_v$1.3_V388C tetrameric channel. Top view of the channel seen from the extracellular side (left), side view of the channel (right). (B), enlargement of the graphs shown in (A) without the highlighted α-pore.

not have contact with the pore. This makes it easy to understand why the electrophysiological data summarized in Table 2 show that the substitution M390F has no influence on σ-current through the mutant channel.

Similarly, position 413, located opposite of C388, has no contact with the σ-pore as shown in Fig. 6*B* independent on whether there is an alanine or a phenylalanine at this position. This explains why we could measure σ-pore current through the *h*K$_v$1.3_V388C_A413F mutant channel (Tab. 2).

Position 392 and 395 in the tetrameric hKv1.3_V388C mutant channel line the σ-pore

Threonine at position 392 seems to line the σ-pore as can be seen in Fig. 6C (*left*). Replacing threonine with the larger tyrosine shown in Fig. 6*C* (*right*) reveals that the large aromatic phenyl group is completely immerged into the σ-pore pathway thereby preventing σ-pore current.

According to the model shown in Fig. 6*D,* Y395 does not seem to be located in the σ-pore, however, seems to have contact to the σ-pore through its phenyl ring and to the cysteine at position 388. The mutation Y395W influenced the σ-pore, because W395 blocked current through the σ-pore in the tetrameric *h*K$_v$1.3_V388C channel. It seems that the pyrrole cycle of the tryptophan at position 395 is closer to C388 compared to the tyrosine at the same position and might therefore more strongly interact with the cysteine 388. That interaction may influence the position of C388 and could therefore lead to the closure of the σ-pore.

Positions 384 and 393 in the tetrameric hK$_v$1.3_V388C mutant channel are far away from the σ-pore

Position 384 is quite remote from the σ-pore and does not come directly in contact with the σ-pore, as can be seen in Fig. 6*E*. Even the enlargement of the side chain of phenylalanine at position 384 by a pyrrole cycle to tryptophan (F384W) did not modify the σ-pore pathway (Fig. 6*E*). Therefore, the σ-pore current was still measurable (Tab. 2).

Position V393 was selected because it is located close to C388 (Fig. 6*F*). We mutated valine to leucine at this position to increase its contact with position C388 in an attempt to affect the σ-pore. This manipulation, however, did neither affect the cysteine at position 388 nor change the current through the σ-pore.

Conclusion

The result of the present study confirms and extends the findings of Prütting and Grissmer [10] who described first that the V388C mutation in *h*K$_v$1.3 channels resulted in a channel with two ion-conducting pathways, the central, potassium selective α-pore and

the σ-pore being open at negative membrane potentials at which the α-pore is normally closed. Our experiments with the trimeric $hK_v1.3\_V388C$ mutant channel showed that the σ-pore was independent of the α-pore and site-directed mutagenesis identified two amino acids in the channel that line the σ-pore (position 392 and 395).

Together with the observation of the σ-pore in a closely related potassium channel ($hK_v1.2\_V370C$) [11] we conclude that the σ-pore may be a structural element common in a variety of voltage-gated ion channels. This in turn, might have implications for the treatment of those ion channel diseases that are associated with mutations in the pore region [14]. For example mutations in HERG channels [15, 16] leading to Na^+ currents might induce long depolarizations and arrhythmias through a current similar to the σ-pore current. In addition, mutations in Ca^{2+} channels could induce migraine through a similar mechanism, i.e. current through a σ-pore. In both cases these diseases should be treated with selective σ-pore blockers, yet to be identified.

Abbreviations

CTX (Charybdotoxin); KTX (Kaliotoxin); MTX (Maurotoxin); wt (wild type).

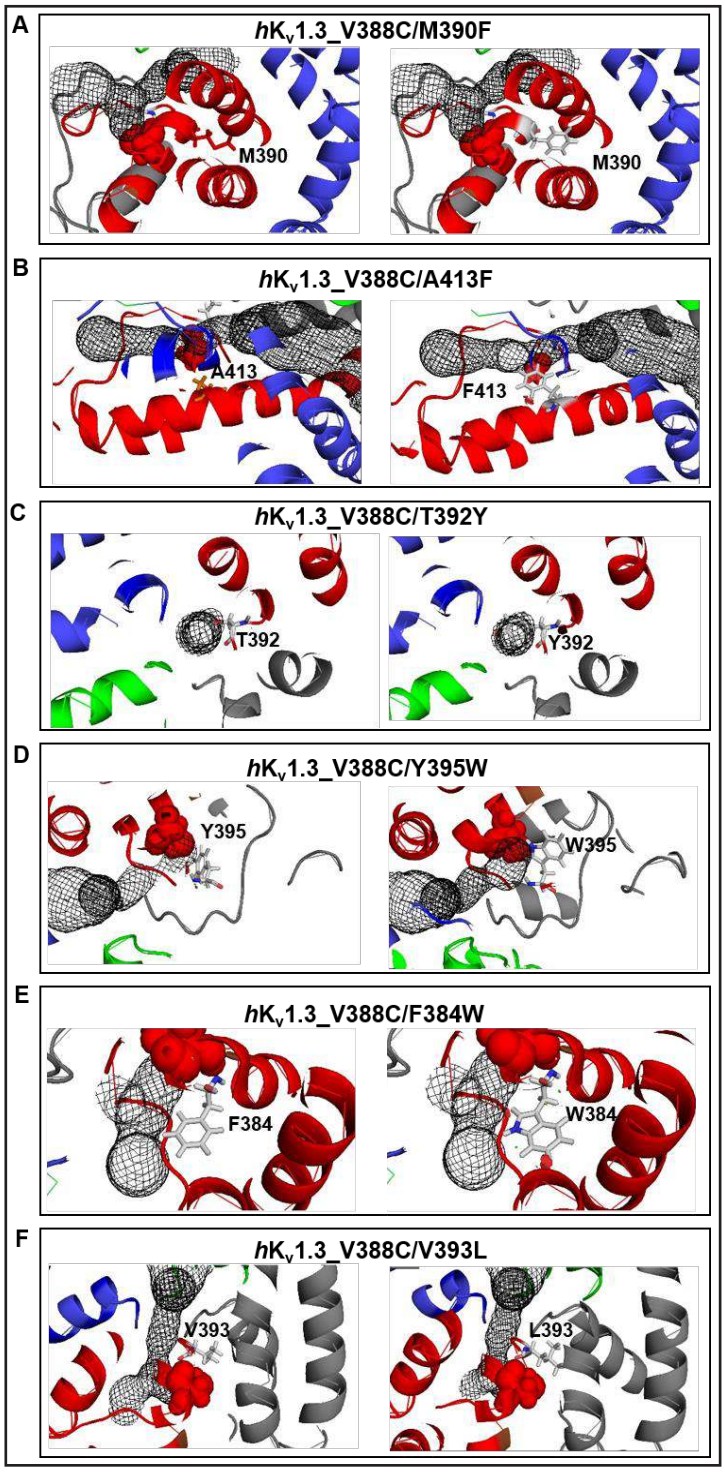

Fig. 6. Region-specific enlargements of the mutated amino acids and the σ-pore in the tetrameric $hK_v1.3\_V388C$ channel. Left columns, wt amino acids; right columns, mutated amino acids. A, $hK_v1.3\_V388C/M390F$; B, $hK_v1.3\_V388C/A413F$; C, $hK_v1.3\_V388C/T392Y$; D, $hK_v1.3\_V388C/Y395W$; E, $hK_v1.3\_V388C/F384W$; F, $hK_v1.3\_V388C/V393L$. The σ-pore is shown in black.

Acknowledgements

This work was supported by a grant from the Deutsche Forschungsgemeinschaft (Grant Number 848/17-1).

PT and SG designed the study; PT performed most of the experiments; PT performed the statistical analysis; and PT and SG wrote the manuscript. All authors discussed and analyzed the results.

Disclosure Statement

No conflict of interests exists.

References

1 Hille B: Ion Channels of Excitable Membranes, ed 3, Sunderland (MA), Sinauer Associates, 2001, pp 131-143.
2 Tombola F, Pathak MM, Isacoff EY: How does voltage open an ion channel? Ann Rev Cell Dev Biol 2006;22:23-52.
3 Doyle DA, Morais Cabral J, Pfuetzner RA, Kuo A, Gulbis JM, Cohen SL, Chait BT, MacKinnon R: The structure of the potassium channel: molecular basis of K^+ conduction and selectivity. Science 1998;280:69–77.
4 Sokolov S, Scheuer T, Catterall WA: Ion permeation through a voltage-sensitive gating pore in brain sodium channels having voltage sensor mutations. Neuron 2005;47:183-189.
5 Sokolov S, Scheuer T, Catterall WA: Gating pore current in an inherited ion channelopathy. Nature 2007;446:76-78.
6 Tombola F, Pathak MM, Isacoff EY: How far will you go to sense voltage? Neuron (2005);48:719-725.
7 Tombola F, Pathak MM, Gorostiza P, Isacoff EY: The twisted ion-permeation pathway of a resting voltage-sensing domain. Nature 2007;445:546-549.
8 Struyk AF, Cannon SC: A Na^+ channel mutation linked to hypokalemic periodic paralysis exposes a proton-selective gating pore. J Gen Physiol 2007;130:11-20.
9 Matthews E, Labrum R, Sweeney MG, Sud R, Haworth A, Chinnery PF, Meola G, Schorge S, Kullmann DM, Davis MB, Hanna MG: Voltage sensor charge loss accounts for most cases of hypokalemic periodic paralysis. Neurology 2009;72:1544-1547.
10 Prütting S, Grissmer S: A novel current pathway parallel to the central pore in a mutant voltage-gated potassium channel. J Biol Chem 2011;286:20031-20042.
11 Tyutyaev P, Grissmer S: Observation of σ-pore currents in mutant *h*Kv1.2_V370C potassium channels. PLoS One 2017 DOI: 10.1371/journal.pone.0176078.
12 Hamill OP, Marty A, Neher E, Sakmann B, Sigworth FJ: Improved patch-clamp techniques for high-resolution current recording from cells and cell-free membrane patches. Pflügers Arch 1981;391:85-100.
13 Rauer H, Grissmer S: The effect of deep pore mutations on the action of phenylalkylamines on the Kv1.3 potassium channel. Br J Pharmacol 1999;127:1065-1074.
14 Lehmann-Horn F, Jurkat-Rott K: Voltage-Gated Ion Channels and Hereditary Disease. Physiol Rev 1999;79:1317-1372.
15 Lees-Miller JP, Duan Y, Teng GQ, Thorstad K, Duff HJ: Novel Gain-of-Function Mechanism in K^+ Channel-Related Long-QT Sydrome: Altered Gating and Selectivity in the HERG1 N269D Mutant. Circulation Res 2000;86:507-513.
16 Teng GQ, Zhao X, Cross JC, Li P, Lees-Miller JP, Guo J, Dyck JR, Duff HJ: Prolonged repolarization and triggered activity induced by adenoviral expression of HERG N629D in cardiomyocytes derived from stem cells. Cardiovascular Res 2004;61:268-277.